Online Resource 1

Joint frequency and voltage support from inverter air-conditioner fleets through network-aware predictive control

Electrical Engineering

Divine Okeke, Elena Gryazina, Federico M. Ibanez, and Yasir Khan

Center for Energy Science and Technology, Skolkovo Institute of Science and Technology, Moscow, Russia

Corresponding author: Divine Okeke Divine.Okeke@skoltech.ru

S1. Model Parameters and Thermal Calibration

The supplementary material provides the numerical assumptions, calibration diagnostics, complete controller comparisons, and supporting dynamic and converter results for the main article. The control architecture is shown in the main manuscript.

Table S1 lists the nominal controller, device, and feeder parameters. The simulations use the effective whole-building thermal model fitted to public National Institute of Standards and Technology (NIST) Net-Zero Energy Residential Test Facility (NZERTF) cooling-season measurements. Table S2 provides the chronological 70/30 holdout and local parameter sensitivities. Table S3 and Fig. S1 report the calibration fit; Fig. S2 shows its residual diagnostics. The fitted thermal resistance, capacitance, and coefficient of performance (RC/COP) provide a reproducible relationship between electrical consumption and indoor temperature. The short calibration window identifies cooling and internal heat gains more strongly than thermal capacitance. In the lower block of Table S2, the two columns report RMSE changes after -10% and $+10\%$ parameter perturbations, respectively.

Table S4 and Fig. S3 illustrate the calibration workflow on simulated data from ResStock and EnergyPlus. All 26 grid-support scenarios use the NIST parameters.

Table S1 Simulation and controller parameters after NIST measured-data calibration

Quantity	Symbol	Value
Nominal frequency	f_0	60 Hz
MPC sample time	T_s	5 s
MPC horizon	M	12 steps
IAC set power	P_{set}	2.0 kW/unit
Compressor range	P_{min}, P_{max}	0.6, 3.5 kW
Inverter rating	S_{rated}	4.0 kVA/unit
Reactive limit	Q_{max}	2.2 kvar/unit
Current-loop bandwidth	f_{ci}	18 Hz
Thermal setpoint	T_{set}	23.42 °C
Thermal resistance	R_{th}	11.47 °C/kW
Thermal capacitance	C_{th}	80.0 kWh/°C
Nominal COP	COP	1.53
Comfort band	ΔT	±1 °C nominal
Nominal fleet size	N	500 units

Table S2 NIST NZERTF holdout check and local parameter sensitivity

Diagnostic	Train	Test
Samples	14093	6040
Indoor RMSE (°C)	0.115	0.173
Indoor MAE (°C)	0.078	0.142
Bias (°C)	-0.002	-0.135
Parameter perturbation	−10%	+10%
R_{th} RMSE change (°C)	0.014	0.005
C_{th} RMSE change (°C)	0.001	0.000
COP RMSE change (°C)	0.156	0.140
COP slope RMSE change (°C)	0.002	0.000
Internal gain RMSE change (°C)	0.103	0.117

Table S3 NIST NZERTF measured-data thermal calibration

Quantity	Value
Measured data year	2015
Fit window	2015-07-19–2015-08-01
Samples / cooling samples	20133 / 13286
Indoor-temperature RMSE	0.114 °C
Active-cooling RMSE	0.130 °C
R_{th}, C_{th}	11.470 °C/kW, 80.0 kWh/°C
COP and lift slope	1.533, -0.0287 per °C

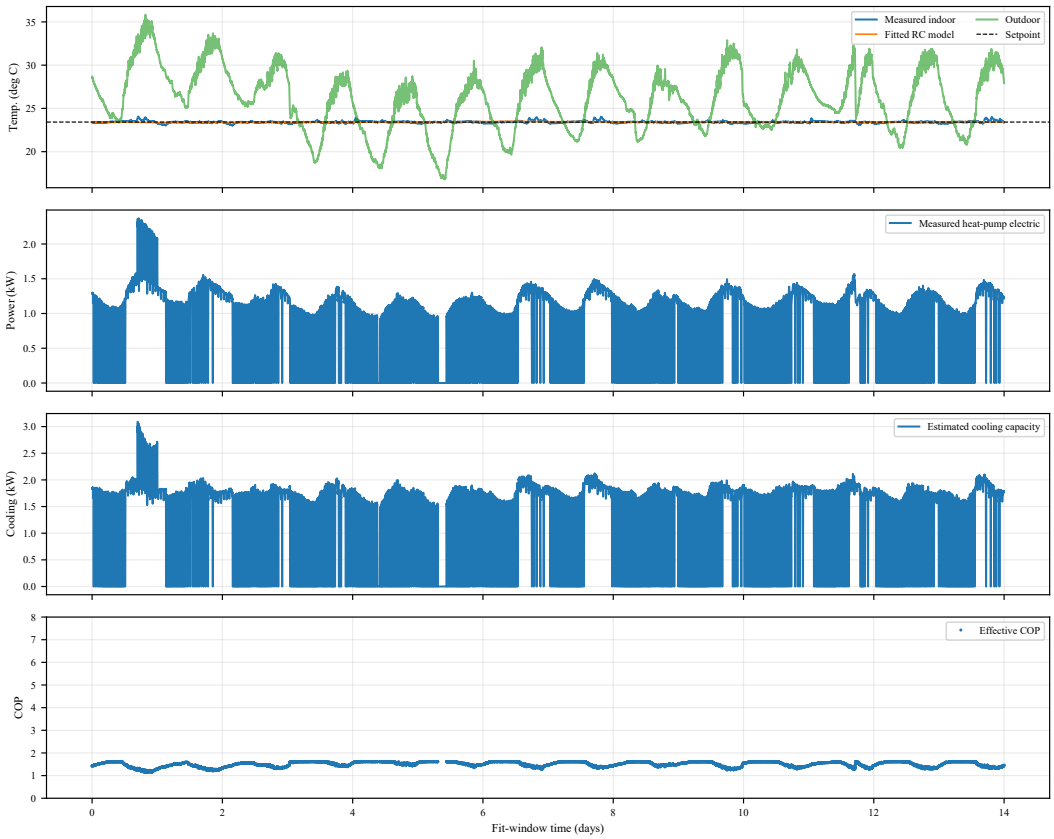


Fig. S1 NIST NZERTF measured-data calibration window. The fitted effective resistance-capacitance/coefficient-of-performance (RC/COP) model is calibrated against test-house indoor temperature, outdoor temperature, measured heat-pump electric power, and cooling intervals inferred from heating, ventilation, and air-conditioning (HVAC) supply/return air measurements

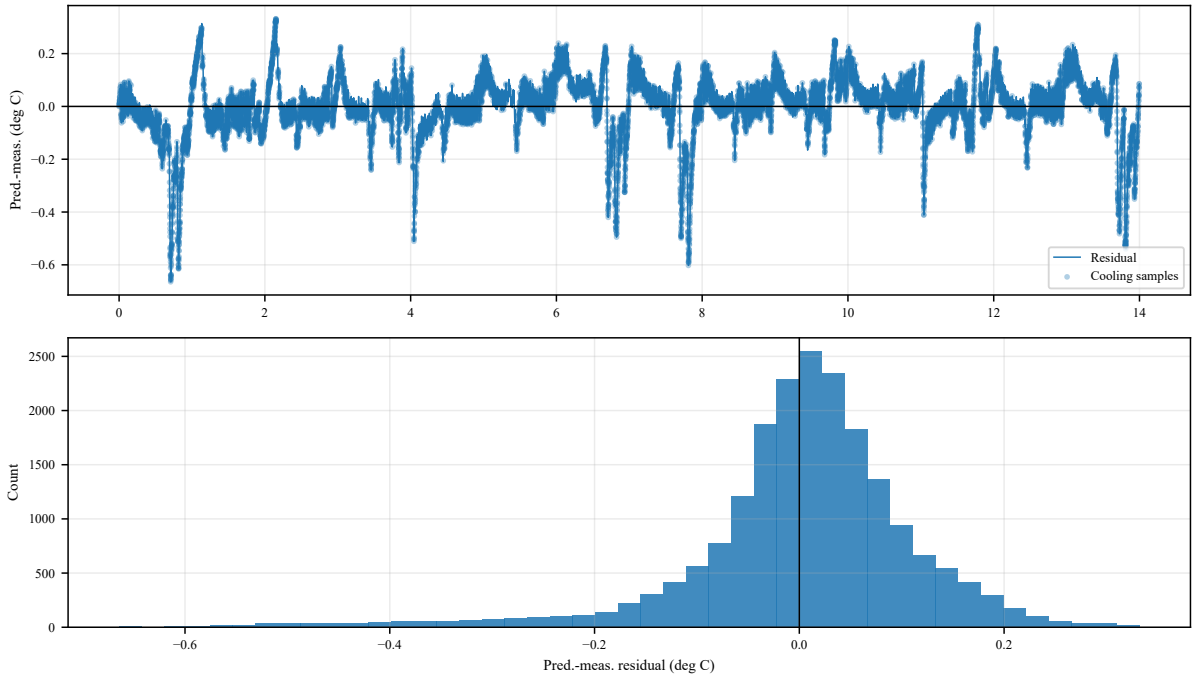


Fig. S2 NIST NZERTF calibration residual diagnostics. The chronological residual trace and histogram show the prediction-minus-measurement indoor-temperature error over the same cooling-season calibration window used for the fitted effective RC/COP model

Table S4 ResStock/EnergyPlus calibration case and fitted parameters

Quantity	Value
Dataset building	TX 100025
Location/weather	TX, Pflugerville; Austin Camp Mabry
Building type	Single-Family Detached, 1698 ft^2
Cooling system	Central AC, SEER 15
Fit window	2018-07-18–2018-07-31
Indoor-temperature RMSE	0.102 °C
R_{th}, C_{th}	2.716 °C/kW, 40.0 kWh/°C
COP and lift slope	3.466, -0.0192 per °C

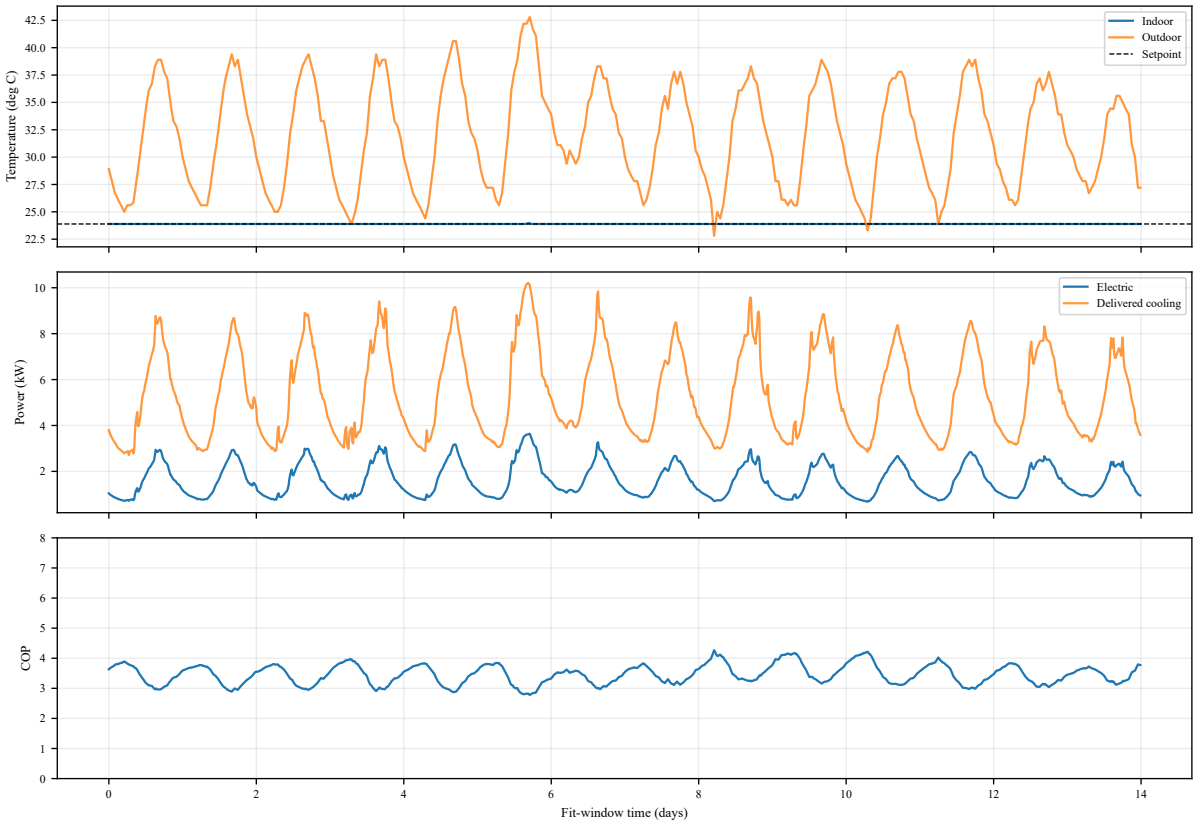


Fig. S3 ResStock/EnergyPlus comparison calibration retained as a simulated-data benchmark for the measured-data calibration workflow

Rule-based frequency response

Inside the comfort band, define $h = (T_{in} - T_{\min})/(T_{\max} - T_{\min})$ and the saturated frequency-response factor

$$r = \min\{\max[(|\Delta f| - 0.03)/0.27, 0], 1\}.$$

For underfrequency the active command is $P_{\text{set}} - r(1-h)(P_{\text{set}} - P_{\min})$; for overfrequency it is $P_{\text{set}} + rh(P_{\max} - P_{\text{set}})$. The command is P_{set} within the ± 0.03 Hz deadband. At $T_{in} \geq T_{\max}$ the command is $P_{\max}$, and at $T_{in} \leq T_{\min}$ it is $P_{\min}$, overriding frequency service. These commands pass through the same downstream ramp and inverter limits as the other controllers. At the midpoint of a symmetric comfort band, half of the available upward or downward power range is eligible for frequency response.

S2. Representative Closed-Loop Cases

Table S5 summarizes all 26 scenarios, comprising deterministic sweeps and three stochastic diagnostic cases. Each frequency or voltage entry is the arithmetic mean of the corresponding full-trajectory minimum across scenarios. $V_{\min}$ denotes the minimum over feeder bus-phase voltages; V_{PCC} denotes the minimum fleet-weighted connection-point voltage. Controller time is the mean of scenario-mean timings, including sensitivity estimation and optimization but excluding downstream plant advancement. Comfort entries give the mean count of samples outside the modeled temperature band. Energy and capacitive-reactive totals in Online Resource 2 use left-held power over each recorded interval; violation degree-minutes use trapezoidal integration of sampled temperature violations.

Table S6 gives the source-sag, feeder-stress, inverter-headroom, and thermostatically controlled load (TCL)-share cases. Its extrema cover the complete 0–600 s trajectories, including the pre-event and recovery periods. The full-amplitude voltage event spans 180–380 s, followed by half-load or 0.985 pu source recovery until 460 s before full restoration. The frequency disturbance spans 120–420 s. Fig. S4 shows how reactive support improves the fleet-weighted voltage while an upstream sag continues to depress the feeder minimum.

Table S5 Mean performance across 26 NIST-calibrated scenarios. Frequency and voltage entries average full-trajectory minima; controller time averages the scenario means.

Controller	$f_{\min}$ (Hz)	$V_{\min}$ (pu)	V_{PCC} (pu)	Comfort viol.	Time (ms)
No support	59.805	0.9001	0.9399	0.0	0.0
Rule based	59.805	0.9126	0.9509	0.0	0.0
MPC-P	59.899	0.9117	0.9462	0.0	228.6
MPC-P+VV	59.899	0.9176	0.9535	0.0	228.3
Full P/Q MPC	59.901	0.9215	0.9704	0.0	539.4

Table S6 Representative scenarios: extrema over each complete simulation trajectory, including the pre-event and recovery intervals.

Scenario	Controller	$f_{\min}$ (Hz)	$V_{\min}$ (pu)	V_{PCC} (pu)	$Q_{\max}$ (kvar)
voltage_sag_0.92	No support	59.805	0.8988	0.9396	0.0
voltage_sag_0.92	Rule based	59.805	0.9115	0.9503	1066.6
voltage_sag_0.92	MPC-P	59.910	0.9109	0.9464	0.0
voltage_sag_0.92	MPC-P+VV	59.910	0.9193	0.9541	925.0
voltage_sag_0.92	Full P/Q MPC	59.910	0.9199	0.9716	1100.0
feeder_stress_1200kw_600kvar	No support	59.805	0.9274	0.9784	0.0
feeder_stress_1200kw_600kvar	Rule based	59.805	0.9302	0.9801	0.0
feeder_stress_1200kw_600kvar	MPC-P	59.910	0.9383	0.9838	0.0
feeder_stress_1200kw_600kvar	MPC-P+VV	59.910	0.9383	0.9838	0.0
feeder_stress_1200kw_600kvar	Full P/Q MPC	59.910	0.9499	0.9943	1100.0
headroom_1.50pu	No support	59.805	0.8988	0.9396	0.0
headroom_1.50pu	Rule based	59.805	0.9040	0.9434	1599.9
headroom_1.50pu	MPC-P	59.910	0.9109	0.9464	0.0
headroom_1.50pu	MPC-P+VV	59.910	0.9125	0.9478	1387.5
headroom_1.50pu	Full P/Q MPC	59.910	0.9199	0.9847	1650.0
tcl_share_40pct	No support	59.805	0.8921	0.9359	0.0
tcl_share_40pct	Rule based	59.805	0.9029	0.9445	1524.6
tcl_share_40pct	MPC-P	59.909	0.9089	0.9453	0.0
tcl_share_40pct	MPC-P+VV	59.909	0.9129	0.9489	1324.3
tcl_share_40pct	Full P/Q MPC	59.932	0.9199	0.9805	1524.6

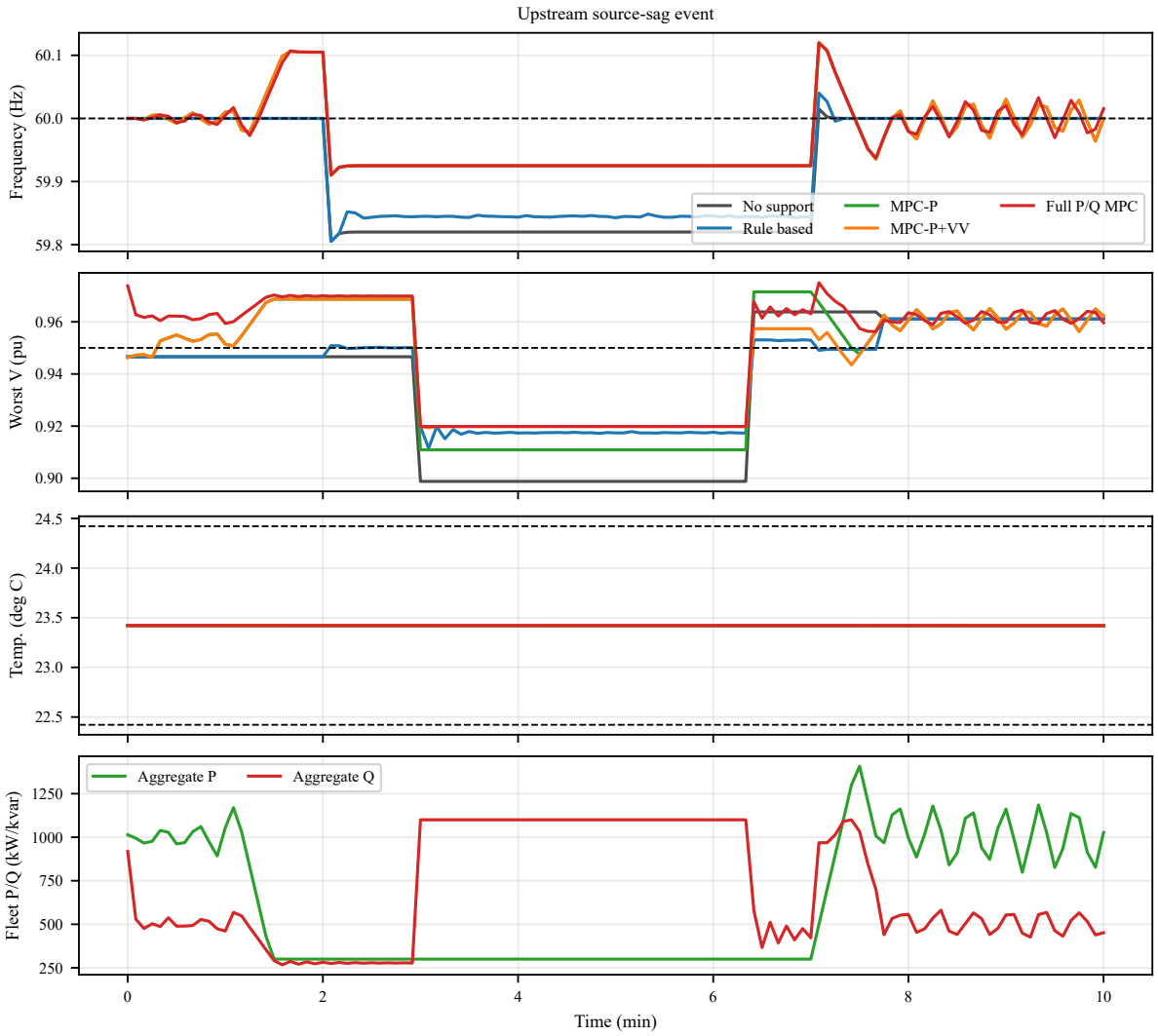


Fig. S4 Controller comparison for the upstream source-sag event. Full P/Q MPC improves frequency and fleet-weighted voltage, but worst-bus voltage recovery is limited by the source-side disturbance and finite inverter rating

S3. Headroom and Optimal-Power-Flow Sensitivity Diagnostics

Fig. S5 shows source-sag voltage recovery as inverter kVA, kvar, RMS-current, and DC-link-current limits are increased together. Table S7 gives the targeted shared-P/Q rating ablation from the feeder-stress case; its trajectories appear in the main article. Table S8 compares the local optimal-power-flow (OPF) sensitivity prediction against nonlinear OpenDSS power flow after applying the corresponding P/Q setpoint.

The targeted ablation changes only the apparent-power rating.

Utilization is $\sqrt{P^2 + Q^2}/S_{\text{rated}}$; the recorded near-binding criterion is utilization ≥ 0.99. It identifies 10 samples in the 2.6 kVA case and none in the 4.0 or 6.0 kVA cases. Active-ceiling loss is

$$\min(P_{\max}, S_{\text{rated}}) - \min(P_{\max}, \sqrt{S_{\text{rated}}^2 - Q^2}).$$

This measures the reduction in feasible active power, which need not constrain the chosen compressor trajectory. All ablation extrema cover the complete trajectories.

Table S7 Shared P/Q headroom ablation for the 1200 kW/600 kvar feeder-stress case. The last column is the maximum reduction in the active-power ceiling caused by the simultaneous reactive-power command, relative to the no-kvar ceiling for the same apparent-power rating.

Case	S kVA	$\min V$ pu	$f_{\min}$ Hz	$Q_{\max}$ kvar	max util. pu	max $\Delta P_{\max}(Q)$ kW/IAC
finite 2.6 kVA	2.6	0.9452	59.910	990	1.000	0.92
nominal 4.0 kVA	4.0	0.9499	59.910	1100	0.867	0.16
relaxed 6.0 kVA	6.0	0.9499	59.910	1100	0.578	0.00

Table S8 Sensitivity OPF prediction versus OpenDSS power-flow check

Scenario	V_{OPF} (pu)	V_{DSS} (pu)	Error (pu)
Source sag	0.9367	0.9199	+0.0168
Feeder stress	0.9480	0.9484	-0.0004

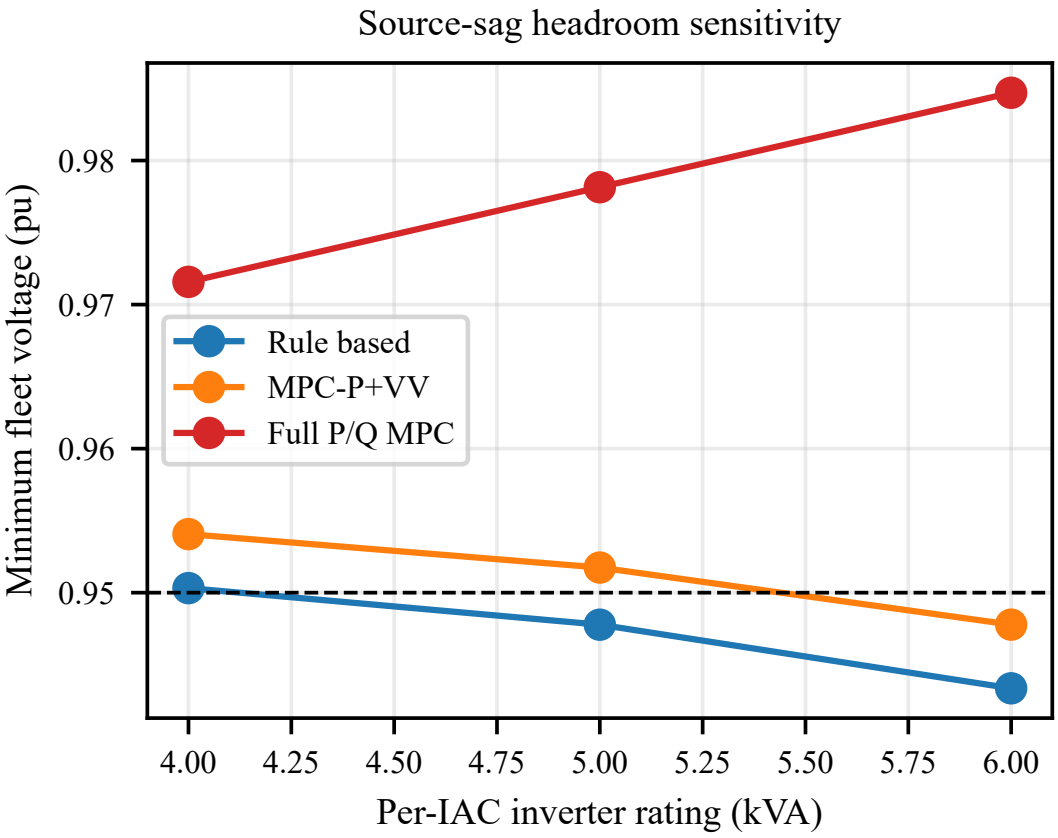


Fig. S5 Fleet-weighted voltage sensitivity to physically explicit inverter kVA/Q/current headroom during source sag

S4. Dynamic, T&D, and Converter Evaluation

The dynamic and converter studies evaluate frequency response, transmission–distribution feedback, and P/Q tracking at complementary physical scales. They use coordinated representative source-sag-family inputs, with the fast converter test adding its specified voltage notch and frequency pulse.

S4.1. Nonlinear frequency response

Fig. S6 and Table S9 compare the replay and nonlinear transmission-dynamic frequency responses to active-power relief. The nonlinear transmission model evaluates the frequency benefit of active-power relief, complementing the reactive-voltage response established by the unbalanced feeder studies.

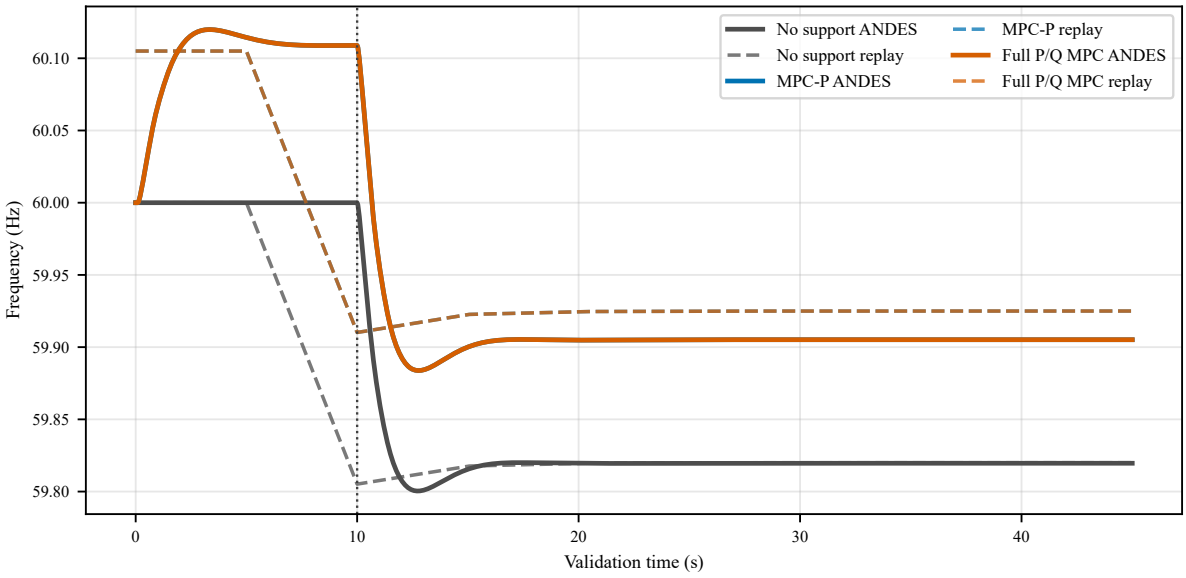


Fig. S6 Nonlinear transmission-dynamic frequency check on the IEEE 14-bus benchmark. Solid curves are center-of-inertia frequency; dashed curves are the dynamic replay traces over the same event window

Table S9 Nonlinear ANDES IEEE 14-bus transient-stability check of active-power frequency support.

Controller	ANDES nadir (Hz)	Replay nadir (Hz)	Error (Hz)	IAC relief (kW)
No support	59.800	59.805	0.005	0
MPC-P	59.884	59.910	0.026	714
Full P/Q MPC	59.884	59.910	0.026	714

S4.2. Transmission–distribution feedback

Fig. S7 and Table S10 report the explicit loose-coupled transmission-and-distribution (T&D) study. Interface voltage and feeder boundary load are exchanged every 100 ms. The full P/Q case improves voltage and frequency relative to no support, while its frequency nadir is 0.012 Hz below active-only MPC in this coupled case.

Table S10 Explicit loose-coupled T&D consistency check with ANDES IEEE 14-bus and OpenDSS IEEE 13-node systems.

Controller	Nadir (Hz)	$V_{\min}$ (pu)	PCC V (pu)	Max. boundary load (kW)
No support	59.826	0.8988	0.9396	4628
MPC-P	59.904	0.9095	0.9449	3888
Full P/Q MPC	59.892	0.9185	0.9700	3889

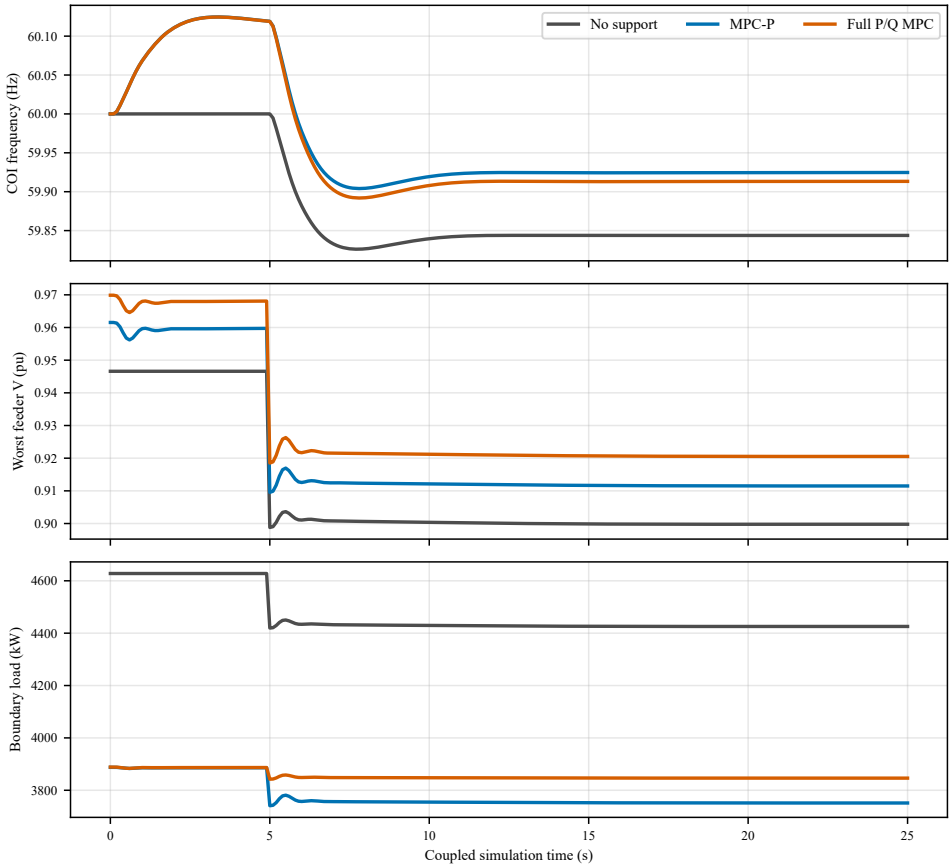


Fig. S7 Explicit loose-coupled T&D consistency check with nonlinear transmission dynamics and unbalanced feeder feedback at every 100 ms macro-step

S4.3. Averaged and Switching Converter Tracking

Figs. S8 and S9 assess representative P/Q tracking, current, and DC-link behavior. Tables S11 and S12 collect the metrics for the two models. The switching simulation uses a 20 μs step and 10 kHz pulse-width modulation (PWM). Its P/Q errors and 4.72 A maximum RMS current describe the fundamental component; the 37.75 A instantaneous peak includes reconstructed switching ripple. The reported RMS current is $\sqrt{i_d^2 + i_q^2}$ and excludes that ripple.

Table S11 Averaged converter trackability-check metrics for the full P/Q MPC trajectory.

Metric	Value
Maximum $\lvert P - P^\star \rvert$	0.467 kW
RMS P error	0.367 kW
Maximum $\lvert Q - Q^\star \rvert$	1.488 kvar
RMS Q error	0.117 kvar
Maximum RMS current	13.31 A
Minimum DC-link voltage	388.6 V
Current saturation fraction	0.00%
Maximum PLL frequency error	0.329 Hz

Table S12 Switching-level inverter trackability-check metrics for the full P/Q MPC trajectory.

Metric	Value
Switching step	20.0 μs
PWM switching frequency	10.0 kHz
RMS P tracking error	0.012 kW
RMS Q tracking error	0.010 kvar
Maximum fundamental RMS current	4.72 A
Peak instantaneous AC current	37.75 A
Minimum DC-link voltage	389.2 V
Voltage saturation fraction	0.00%
Maximum PLL frequency error	1.650 Hz

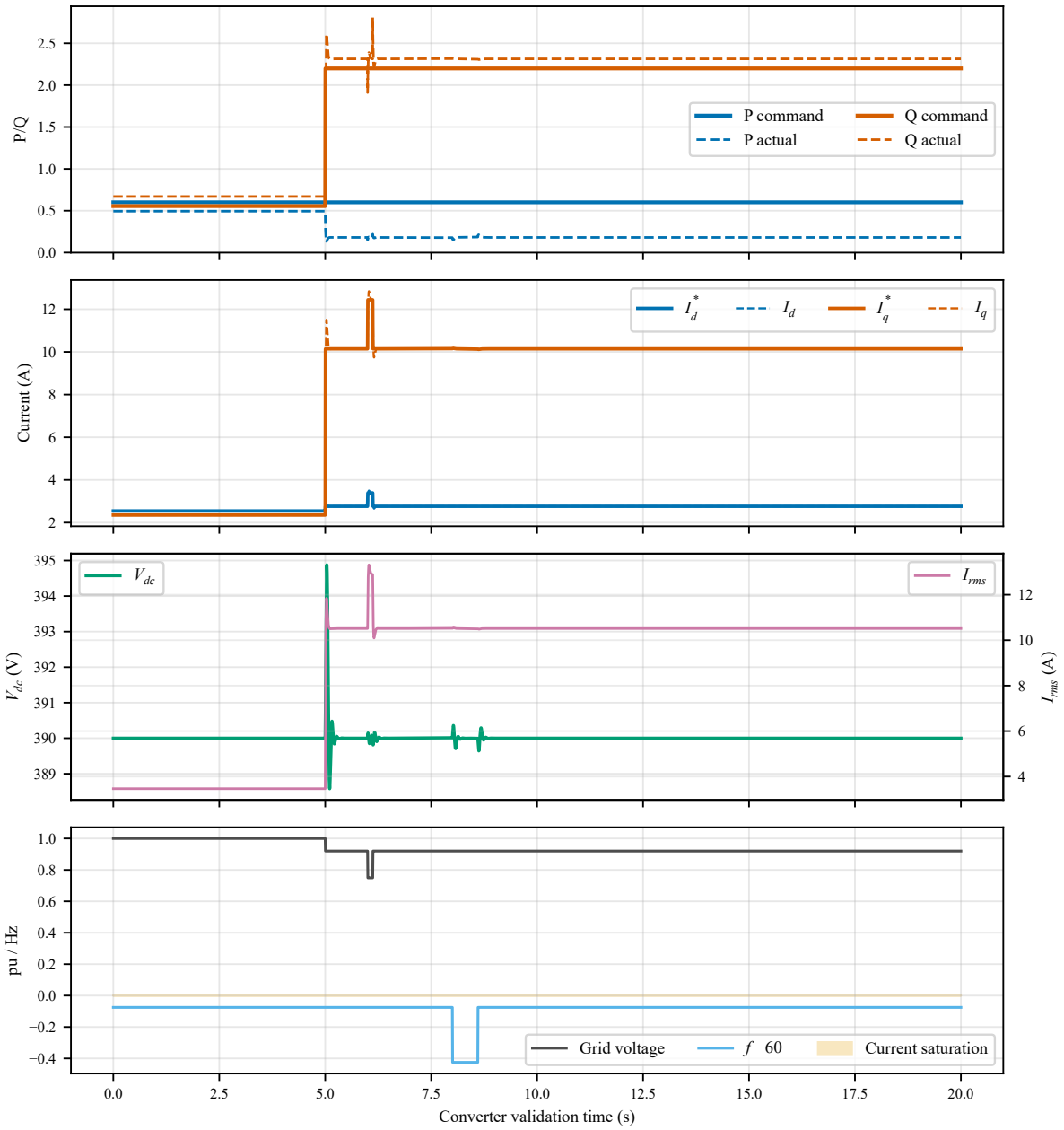


Fig. S8 Averaged inverter trackability check for the full P/Q network-aware fleet model predictive controller (MPC) trajectory. The model includes phase-locked-loop (PLL) dynamics, dq current proportional-integral (PI) control, L-filter dynamics, pulse-width-modulation (PWM) delay, direct-current (DC)-link capacitance, current limiting, and anti-windup

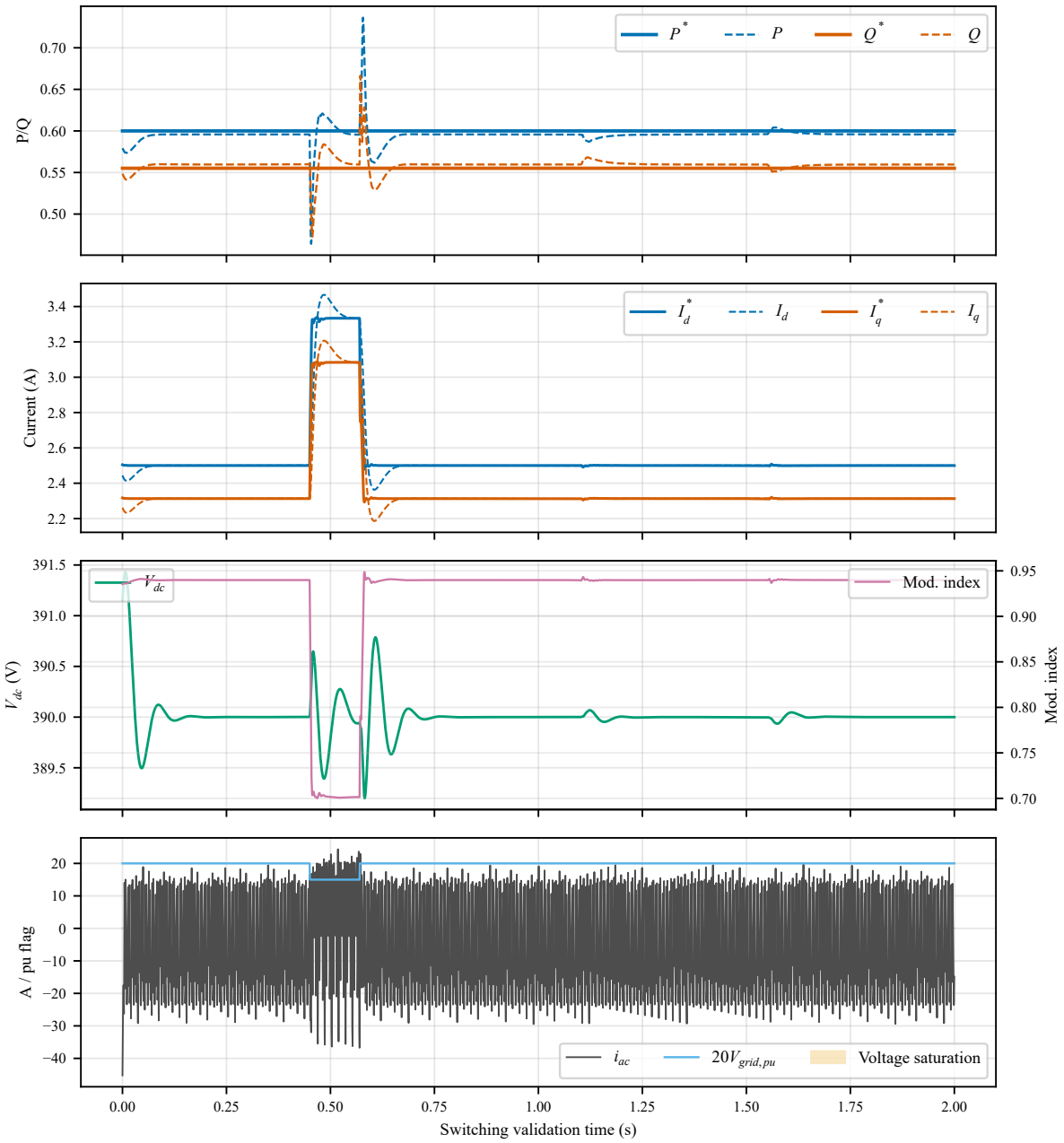


Fig. S9 Switching-level trackability check of one representative inverter-based air-conditioner (IAC) inverter connected to a Thevenin-equivalent feeder bus. The slow reference is the full P/Q MPC command trajectory. The fast layer combines fundamental dq dynamics with explicit PWM ripple reconstruction, PLL synchronization, DC-link dynamics, and current/voltage saturation logic. The reported RMS-current metric represents the fundamental component